

STRUCTURAL, MORPHOLOGICAL AND OPTICAL INVESTIGATIONS OF SILVER NANOPARTICLES SYNTHESIZED BY SOL-GEL AUTO-COMBUSTION METHOD

A. AZIZ^a, M. KHALID^{b,*}, M. SAEED AKHTAR^c, M. NADEEM^d,
Z. A. GILANI^b, H. M. N. UL HUDA KHAN ASGHAR^b, J. REHMAN^b,
Z. ULLAH^e, M. SALEEM^f

^aDepartment of Physics, NED University of Engineering and Technology, 75270, Karachi, Pakistan

^bDepartment of Physics, Balochistan University of Information Technology, Engineering and Management Sciences, Quetta, 87300, Pakistan

^cDepartment of Physics, Division of Science and Technology, University of Education, College Road, Township, Lahore, Pakistan

^dDepartment of Basic Sciences and Humanities, University of Engineering and Technology, 47050, Taxila, Pakistan

^eCentre of Excellence in Solid State Physics, University of the Punjab, Lahore-54590, Pakistan

^fDepartment of Physics, School of Sciences and Engineering (SSE), Lahore University of Management Sciences (LUMS), Lahore, Pakistan

Effect of post-synthesis annealing temperature on the structural, morphological and optical properties of silver (Ag) nanoparticles has been investigated. Silver nanoparticles have been synthesized by sol-gel auto-combustion method. X-ray diffraction analysis revealed that synthesized nanoparticles exhibit face-centered cubic structure with preferred orientation along (111) plane. Crystallite size has been observed to increase from 22 to 32 nm as the annealing temperature upsurge from 350 to 550 °C. The crystal growth as a result of high annealing temperature has been observed with slight shift in most intense diffraction peak toward smaller 2θ values. As the silver lattice grow with temperature, the lattice stain decreases due to larger grain boundaries. The optical studies revealed that silver nanoparticles exhibit a direct band gap of 2.51 eV. These large band gap silver nanoparticles when embedded in ceramics and glass would have potential applications in optoelectronic devices.

(Received May 5, 2018; Accepted July 24, 2018)

Keywords: Sol-gel preparation, Nanocrystalline materials, Thermal annealing, Structural, Band gap, Grain boundaries

1. Introduction

Metallic nanoparticles have gained an enormous research interest in the last few decades owing to their potential use in diverse industrial applications from catalysis to biomedicine. Nanoparticles exhibit novel (size and shape dependent) properties compared to their bulk counterpart owing to high surface to volume ratio. Among nanoparticles of noble metals, silver nanoparticles have been studied extensively for their commercial application in variety of industries specifically in nanomedicine [1]. The characteristics of nanoparticles principally depend on the synthesis procedure in addition to the selection of precursors and chelating/reducing agents [2]. There are several chemical, physical and biological methods reported to date for controlled synthesis of silver nanoparticles including evaporation condensation method [3], chemical reduction [4, 5], sol-gel [2, 6], laser ablation [7], electron irradiation [8], gamma irradiation [9], microwave processing [10], electrochemical [11], photochemical [12], successive ionic layer

*Corresponding author: khalid_pu@hotmail.com

deposition (SILD) [13], bromide-mediated polyol method [14], green synthesis [15] and biosynthesis [16, 17]. Among these, sol-gel is a simple and cost-effective method.

Herein, we report the synthesis of silver nanoparticles by sol-gel auto-combustion method and investigate the structural, morphological and optical properties.

2. Materials and methods

All reagents, silver nitrate, lactic acid and poly N- vinylpyrrolidone were purchased from Sigma-Aldrich and used without further purification. De-ionized water was used as a solvent.

The XRD analysis of silver nanoparticles was carried out using Bruker D8 Advance X-ray diffractometer (Germany). Surface morphology of the samples was observed through Scanning Electron Microscope (SEM, S-3400, 20 kV) and the optical properties were obtained after recording absorption spectra from Spectroscopic Ellipsometer.

Silver nitrate (0.04 g), lactic acid (0.2 g) and PVP (0.1 mol/L) were dissolved in de-ionized water under vigorous stirring and final volume of the solution was made up as 100 mL by adding appropriate amount of de-ionized water. Lactic acid and PVP perform the roles of stabilizing and reducing agents, respectively during synthesis of silver nanoparticles. The reaction mixture having pH value of 2 was kept at 80° under magnetic stirring. At initial stages of the reaction, the color of solution changed from white to yellowish due to formation of colloidal suspension of silver nanoparticles. As the reaction proceeds, the solution was transformed to dense black gel. Gel was then taken from the reaction container and dried at 150 °C. Powder samples were then annealed in Ar atmosphere for three hours in muffle furnace at temperatures from 350-550 °C with step of 50 °C before further characterization.

3. Results and discussion

X-ray diffraction patterns of annealed samples are shown in Fig. 1. The XRD patterns reveal that synthesized silver nanoparticles exhibit polycrystalline nature with cubic phase. The observed diffraction peaks correspond to (111), (200), (220) and (311) planes and are well matched with standard data of face centered cubic silver (JCPDS Card No. 04-0783) and literature [5, 18]. The crystallite size was estimated by Scherrer's formula (given below) for all the samples and observed a slight increase in crystallite size with annealing temperature.

$$d = \frac{0.9\lambda}{\beta \cos\theta} \quad (1)$$

where $K = 0.9$ (constant), $\lambda = 1.54 \text{ \AA}$, β is the Full Width at Half Maximum (FWHM) calculated in radians and θ is Bragg's diffraction angle. It is well-known that post heat treatment will improve the crystal structure in terms of grain growth which is evident from increase in d-spacing of the annealed samples from 2.34 to 2.36 Å as a function of annealing temperature [18]. However, the grain growth doesn't significantly affect the crystal phase *i.e.* silver nanoparticles are observed to be grown with stable cubic phase even at high annealing temperature of 550 °C. The structural parameters obtained from XRD data are presented in Table 1.

Table 1. Structural parameters of annealed silver nanoparticles.

Sample No.	Annealing Temp. (°C)	Lattice parameter a (nm)	Crystallite size (nm)	Dislocation density $\times 10^{15}$ (lines/m ²)	Micro strain $\times 10^{-3}$ (lines ² /m ⁴)	Stacking fault
1	350	4.07134	22.37	1.998	1.549	0.4301
2	400	4.07190	28.11	1.265	1.233	0.4301
3	450	4.07579	28.59	1.223	1.212	0.4303
4	500	4.07863	28.71	1.213	1.207	0.4305
5	550	4.08160	32.45	0.949	1.068	0.4307

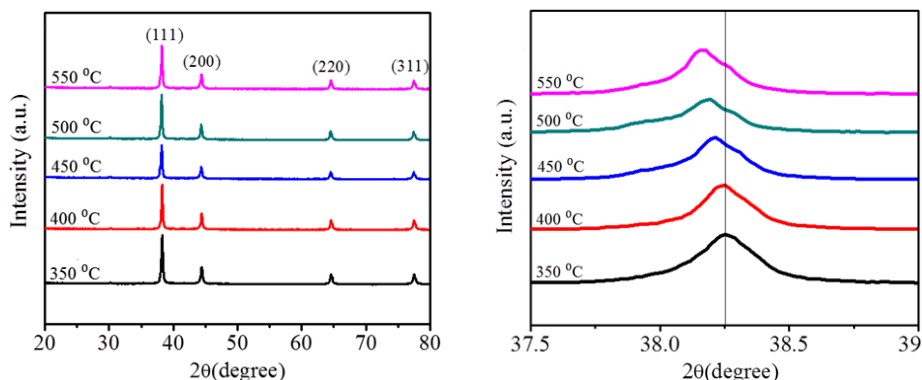


Fig. 1. XRD patterns of silver nanoparticles annealed at various temperatures and A slight shift in most intense diffraction peak (111) showing the grain growth.

The morphology of synthesized silver nanoparticles was observed through Scanning Electron Microscopy and the images are shown in Fig. 2. The SEM images obtained at same magnification for all the samples clearly depict the grain growth as a function of annealing temperature. An agglomerated growth of silver nanoparticles was observed with estimated size of particles ranges from 30 to 150 nm. The grain growth with clear grain boundaries has been observed as the interconnection between small silver nanoparticles vanishes at higher annealing temperatures [19].

The morphology of sample annealed at 550 °C depicts the spherical morphology with clear grain boundaries. However, the agglomeration is still there presenting the key synthesis factor of Sol-Gel Auto-Combustion method. Monodispersed silver nanoparticles can only be obtained by adding surfactants in reaction precursors or by preparing the dilute dispersed solution of these particles under vigorous ultra-sonication for long period of time [15, 20]. The optical properties have been observed by obtaining the absorption spectra [21] from spectroscopic Ellipsometry in the range wavelength from 200-800 nm [22]. The absorption co-efficient related to the optical band gap has been calculated by the relation as;

$$\alpha = \left(\frac{k}{h\nu} \right) (h\nu - E_g)^n \quad (2)$$

where k is a constant, $h\nu$ is the photon energy, h is Planck's constant and n is a number that describes electronic transition between valance and conduction bands with its nature [23]. The variation in $(\alpha h\nu)^2$ as a function of photon energy $h\nu$ is shown in Fig. 3. The linear portion of the curve observed at higher energies was extrapolated towards energy axis in order to evaluate the energy gap of silver nanoparticles. The estimated value of band gap is 2.5 eV.

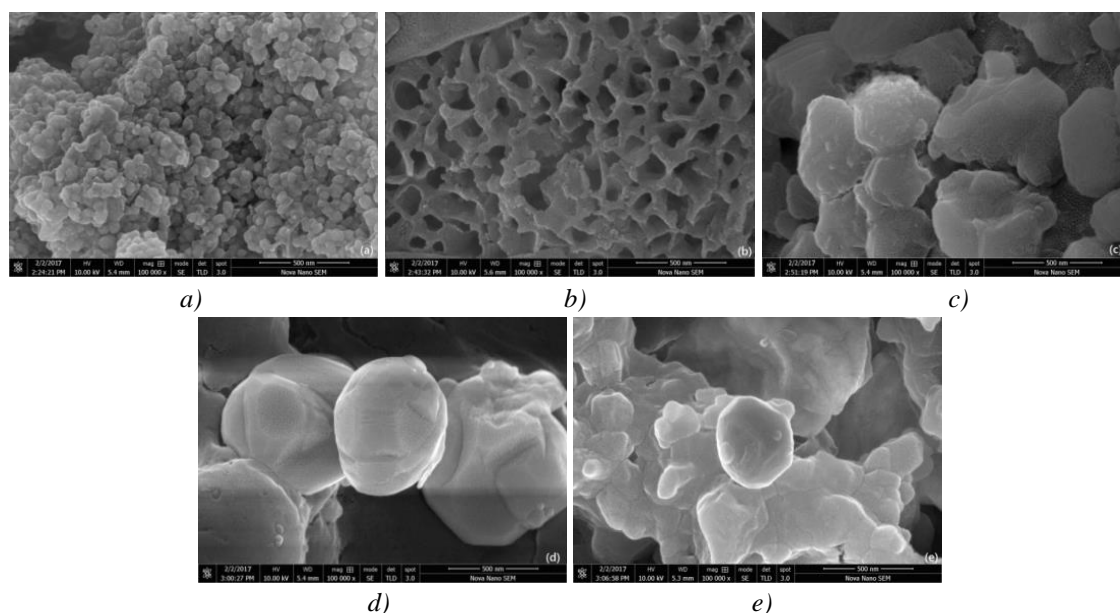


Fig. 2. SEM images of the silver nanoparticles annealed at (a) 350 (b) 400 (c) 450 (d) 500 and (e) 550 °C

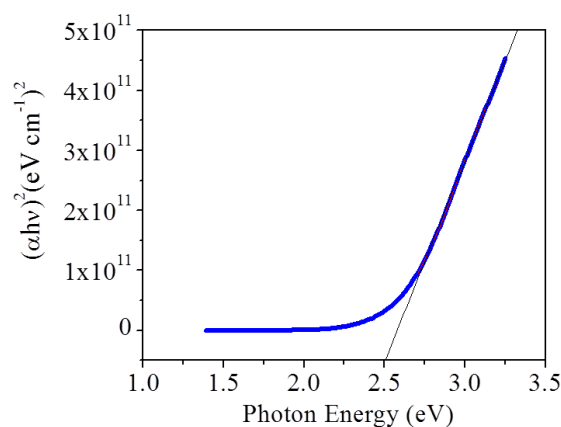


Fig. 3. Band gap plot of silver nanoparticles annealed at 550 °C.

These pure silver nanoparticles with large value of band gap might have applications in advanced optoelectronic devices and sensors [20].

4. Conclusions

Silver nanoparticles were prepared with sol-gel auto-combustion method. The influence of annealing temperature on structural and morphological properties has been investigated. Annealing temperature doesn't significantly affect the crystal phase of nanoparticles, however the grain growth observed as function post heat treatment. The observed band gap (2.5 eV) of silver nanoparticles would make them a suitable candidate for optoelectronic devices and sensors.

References

- [1] J. S. Kim, et al., *Biology and Medicine*, **3**(1), 95 (2007).
- [2] P.-W. Wu, et al., *Journal of Sol-Gel Science and Technology* **19**(1), 249 (2000).

- [3] J. H. Jung, et al., *Journal of Aerosol Science* **37**(12), 1662 (2006).
- [4] M. G. Guzmán, J. Dille, S. Godet, *Int. J. Chem. Biomol. Eng.* **2**(3), 104 (2009).
- [5] W. Shen, et al., *Materials Letters* **213**, 7 (2018).
- [6] N. Lkhagvajav, et al., *Dig. J. Nanomater. Biostruct.* **6**(1), 149 (2011).
- [7] T. Tsuji, et al., *Applied Surface Science* **254**(16), 5224 (2008).
- [8] K. Bogle, S. Dhole, V. Bhoraskar, *Nanotechnology*, **17**(13), 3204 (2006).
- [9] Y. Rao, et al., *Radiation Physics and Chemistry* **79**(12), 1240 (2010).
- [10] H. Yin, et al., *Materials chemistry and Physics* **83**(1), 66 (2004).
- [11] R. A. Khaydarov, et al., *Journal of Nanoparticle Research* **11**(5), 1193 (2009).
- [12] K. G. Stamplecoskie, J. C. Scaiano, *Journal of the American Chemical Society* **132**(6), 1825 (2010).
- [13] I. Kodintsev, V. Tolstoy, A. Lobinsky, *Materials Letters* **196**(Supplement C), 54 (2017).
- [14] P. Zhang, et al., *Materials Letters* **213**, 23 (2018).
- [15] V. Ravichandran, et al., *Materials Letters* **180**(Supplement C), 264 (2016).
- [16] N. Saifuddin, C. Wong, A. Yasumira, *Journal of Chemistry* **6**(1), 61 (2009).
- [17] V. K. Sharma, R. A. Yngard, Y. Lin, *Advances in Colloid and Interface Science.* **145**(1), 83 (2009).
- [18] Y. Sun, Y. Xia, *Science* **298**(5601), 2176 (2002).
- [19] B. Ingham, et al., *Chemistry of Materials* **23**(14), 3312 (2011).
- [20] D. D. Evanoff, G. Chumanov, *Chem. Phys. Chem.* **6**(7), 1221 (2005).